interaction between the two Cu^{2+} ions analogous to that observed in the EPR spectra of the ferric dihydroxamate complexes.[5]

The room-temperature solution EPR spectra of the complexes were also measured in $CHCl_3$/toluene (1/1) and are shown in Figure 6. The spectra are all superimposable (except that the spectrum of the $n = 5$ complex is reduced in intensity) with $g_{\parallel} \sim 2.11$ and $A_{\parallel} \sim 7.9$ mK. The $M_I = {}^3/_2$ line still shows evidence of some splitting for $n = 6$–10, indicating that the two components can be differentiated even at room temperature, although their spectra are almost superimposable.

In conclusion, the Cu(II) complexes of the series of dihydroxamate ligands $i\text{-}C_3H_7N(O)C({=}O)(CH_2)_nC({=}O)N(O)\text{-}i\text{-}C_3H_7^{2-}$ have been prepared and characterized. For $n = 3$ and 4 the complexes appear to be polymeric. For $n \geq 5$ the complexes are dimeric and appear to exist as two principal geometric isomers in solution.

Acknowledgment. We gratefully acknowledge the deliberate consultation of Professor Brian Hoffman. This research was supported by NIH Grant AI 11744.

Registry No. 1, 103693-86-3; Cu_2L_2 ($n = 4$), 103693-90-9; Cu_2L_2 ($n = 6$), 103693-89-6; Cu_2L_2 ($n = 3$), 103693-91-0; Cu_2L_2 ($n = 8$), 103693-88-5; Cu_2L_2 ($n = 10$), 103693-87-4.

Supplementary Material Available: Table III (anisotropic thermal parameters of non-hydrogen atoms), Table IV (fractional coordinates of hydrogen atoms), Table VII (temperature-dependent magnetic susceptibility data for the complexes Cu_2L_2), and a packing diagram of the Cu_2L_2 dimer for $n = 5$ (4 pages); Table V (structure factor amplitudes) (13 pages). Ordering information is given on any current masthead page.

Contribution from the Institut für anorganische Chemie,
Universität Bern, CH-3000 Bern 9, Switzerland

Optical Spectroscopy as a Structural and Electronic Probe in a Coordination Compound: $[(NH_3)_5CrOHCr(NH_3)_5]Cl_5{\cdot}H_2O$

Hans Riesen and Hans U. Güdel*

Received January 8, 1986

Single crystals of $[(NH_3)_5CrOHCr(NH_3)_5]Cl_5{\cdot}H_2O$ were studied by absorption, Zeeman, and site-selective luminescence spectroscopy in the temperature range 1.5–95 K. The existence of two nonequivalent dimer sites was established, and their orientations in the crystal were determined. Exchange splittings, zero-field splittings, and excited-state g values were determined separately for each site. Nonradiative transfer of excitation energy between inequivalent sites was observed at temperatures above 15 K.

Introduction

Structural and electronic properties of transition-metal complexes are often derived from measurements of their bulk properties in the solid state. X-ray diffraction is the most widely used and, in general, the most powerful technique for obtaining molecular structure information. Measurements of the magnetic susceptibility and, less commonly, the heat capacity are used to derive information about low-lying electronic states. They are particularly useful in spin-crossover situations[1] and for the study of exchange-coupled systems.[2] Bulk techniques require the existence of a reasonable molecular model, which can be fitted to the experimental data. They provide an average picture but no direct access to the molecular properties. In cases of structural disorder, subtle superstructures, or very large unit cells the potential of X-ray diffraction may be greatly reduced. This is particularly true for the elucidation of coordination geometries of active metallic sites in metalloproteins. In this currently very active field of research, spectroscopic techniques play a dominant part in obtaining structural information.[3]

We have chosen a classical coordination compound, the acid rhodo chromium(III) complex, to demonstrate the power of optical spectroscopic techniques for the elucidation of structural and electronic properties. There exist two distinct modifications of acid rhodo chromium (III) chloride, a monohydrate and a dihydrate.[4] Both of these have been structurally characterized. The present study is concerned with the monohydrate, the dihydrate being only used as a reference. There are two conflicting reports of the crystal structure of $[(NH_3)_5CrOHCr(NH_3)_5]Cl_5{\cdot}H_2O$, both based on single-crystal X-ray diffraction measurements. Urushiyama et al.[5] published a very brief note in which they assigned the space group to $P4_12_12$ (or $P4_32_12$) with $a = 16.26$ Å, $c = 14.80$ Å, and eight formula units per cell. Hodgson et al.[6] provided a much more detailed account; they assigned the space group to $P4_2/mnm$ with $a = 16.259$ (7) Å, $c = 7.411(7)$ Å, and four formula units per cell. The latter structure was refined to a conventional R value of 0.077. According to this structure the discrete $[(NH_3)_5CrOHCr(NH_3)_5]^{5+}$ complexes have exact C_{2v} symmetry. The 2-fold molecular axes lie perpendicular to the c axis of the tetragonal crystal. The complexes occupy a 4-fold crystallographic site and are therefore all equivalent. Early and preliminary spectroscopic measurements[7] provided some evidence for the existence of two inequivalent sets of complexes, in contradiction to the X-ray diffraction result.

Modern optical spectroscopic techniques allow a site-selective probing of the molecular properties.[8] The luminescence of each site can be obtained individually by selective excitation using tunable lasers. Alternatively, individual excitation spectra can be obtained by monitoring a narrow emission line of a given set. It is possible to obtain molecular parameter separately for inequivalent sites. Polarized single-crystal spectroscopic data should provide information about electronic excitations as well as molecular orientations. Energy splittings resulting from exchange interactions in the dimeric unit $[(NH_3)_5CrOHCr(NH_3)_5]^{5+}$ are of particular interest in the title compound. Since the bulk magnetic properties[6] are determined by the average electronic ground-state splittings of all the sites in the crystal, the spectroscopic probe is expected to be much more selective and thus more informative. In addition, the presence of nearly but not exactly equivalent sites can be used to investigate the nonradiative intermolecular transfer of electronic excitation energy. In this context the presence of inequivalent sites, which clearly limits the power of bulk techniques, turns out to be an advantage. The title

---

(1) Gütlich, P. *Struct. Bonding (Berlin)* **1981**, *44*, 83.

(2) Willett, R. D., Gatteschi, D., Kahn, O., Eds. *Magneto Structural Correlations in Exchange Coupled Systems*; D. Reidel: Dordrecht, The Netherlands, 1985.

(3) Solomon, E. I.; Wilcox, D. E. in *Magneto Structural Correlations in Exchange Coupled Systems*; Willett, R. D., Gatteschi, D., Kahn, O., Eds.; O. Reidel: Dordrecht, The Netherlands, 1985; p 463.

(4) Engel, P.; Güdel, H. U. *Inorg. Chem.* **1977**, *16*, 1589. The trihydrate of ref 9 is identical to the dihydrate referred to in this work.

(5) Urushiyama, A.; Nomura, T.; Nakahara, M. *Bull. Chem. Soc. Jpn.* **1970**, *43*, 3971.

(6) Veal, J. T.; Jeter, D. J.; Hempel, J. C.; Eckberg, R. P.; Hatfield, W. E.; Hodgson, D. E. *Inorg. Chem.* **1973**, *12*, 2928.

(7) Ferguson, J.; Güdel, H. U.; Puza, M. *Aust. J. Chem.* **1973**, *26*, 13.

(8) Yen, W. M., Selzer, P. M., Eds. *Laser Spectroscopy of Solids*; Springer: West Berlin, 1981.

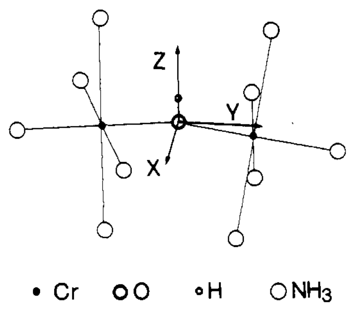

Figure 1. C_{2v} molecular axes in $[(NH_3)_5CrOHCr(NH_3)_5]^{5+}$.

compound was studied by polarized single-crystal absorption and Zeeman spectroscopy as well as site-selective luminescence spectroscopy.

Experimental Section

$[(NH_3)_5CrOHCr(NH_3)_5]Cl_5\cdot H_2O$ as well as $[(NH_3)_5CrOHCr(NH_3)_5]Cl_5\cdot 2H_2O$[4] were prepared by a literature method.[9]

Needlelike crystals of $[(NH_3)_5CrOHCr(NH_3)_5]Cl_5\cdot H_2O$ suitable for single-crystal absorption and Zeeman spectroscopy were obtained by slow evaporation of a saturated solution in 10^{-2} M HCl at room temperature in the dark. From their X-ray powder pattern, which corresponds to the unit cell given in ref 6, as well as the needlelike habitus it was concluded that the crystals were identical with those studied by Hodgson et al.[6] Rectangular plates of $[(NH_3)_5CrOHCr(NH_3)_5]Cl_5\cdot 2H_2O$ were grown at pH 4 and 5 °C.

High-resolution polarized single-crystal transmission experiments were measured as follows: The light of a 150-W quartz–halogen lamp was dispersed by a $^3/_4$-m monochromator (Spex 1702), chopped by a tuning-fork chopper (American Time Products), and polarized by a Rochon prism before passing through the sample. The detection system consisted of a cooled photomultiplier tube (EMI 9659 QB), a preamplifier (PAR 181), and a lock-in amplifier (PAR 186 A). The crystal was cooled by the helium flowtube technique or with a bath cryostat (Oxford Instruments MD4). The same setup was used for the Zeeman measurements, with the sample placed in a cryomagnet (Oxford Instruments, SM4). Temperatures down to 1.5 K with magnetic fields up to 5 T were thus obtained. Site-selective luminescence spectra were excited with a dye laser (Spectra Physics 375; bandwidth 30 GHz; DCM Exciton dye) pumped by an Ar^+ ion laser (Spectra Physics 166; 5 W). The luminescence was dispersed by a 0.85-m double monochromator (Spex 1402) and detected by a cooled PM tube (RCA 31034) in conjunction with a photon-counting system (Spex DPC-2). For luminescence line-narrowing experiments the resolution of the dye laser was improved by a fine-tuning intracavity etalon (Spectra Physics, resulting bandwidth 7 GHz).

A microcomputer (Tektronix 4052A) was used for the data acquisition and all monochromator and dye laser control.

Exchange Coupling and Electronic Excitations

The theory of exchange interactions in chromium (III) dimers, both for the ground state $^4A_2{}^4A_2$ and the singly excited state $^2E^4A_2$, has been treated in detail and will not be repeated here.[10,11] We concentrate on a brief summary of the aspects that are relevant to our discussion.

Figure 1 shows our definition of a molecular Cartesian coordinate system in the rhodo complex.

We represent the exchange coupling in the ground state by the Hamiltonian

$$\hat{H}_g = -2J\vec{S}_1\cdot\vec{S}_2 - j(\vec{S}_1\cdot\vec{S}_2)^2 \qquad (1)$$

with the bilinear and biquadratic exchange parameters J and j, respectively. An appropriate effective Hamiltonian for the singly excited $^2E^4A_2$ state is[10] given by

$$\hat{H}_{ex} = -2\sum_{i,j} J_{ai,bj}\vec{s}_{ai}\cdot\vec{s}_{bj} \qquad (2)$$

where i and j number the singly occupied t_2 orbitals. $J_{ai,bj}$ are orbital exchange parameters. Biquadratic terms are neglected in eq 2. Energies, symmetries, and wave functions of the dimer states are obtained by diagonalizing eq 1 and 2 and using the transformation properties of the molecular point group, C_{2v} in our case.

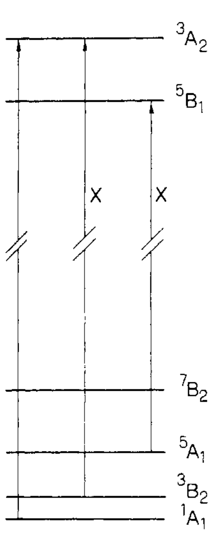

Figure 2. Exchange splitting in the ground state $^4A_2{}^4A_2$ and low-energy part of the $^2E^4A_2$ multiplet. Relevant electronic excitations and polarizations are indicated.

Figure 2 shows the ground-state dimer levels as well as those two levels of the $^2E^4A_2$ excited state that we need for our discussion. $^4A_2 \rightarrow {}^2E$ single excitations in the acid rhodo chromium (III) complex can obtain optical intensity by two possible mechanisms:[11] (i) The first mechanism, a single-ion mechanism, is based on the combined action of the odd-parity ligand field potential at the chromium site and spin–orbit coupling. Both $\Delta S = 0$ and $\Delta S = 1$ transitions, where S is a quantum number representing the total dimer spin, are allowed by this mechanism. (ii) The second is an exchange mechanism, governed by the spin-selection rules $\Delta S = 0$ and $\Delta M_s = 0$ and the orbital selection rules for allowed transitions. Relative intensities and polarizations for the various $^4A_2{}^4A_2 \rightarrow {}^2E^4A_2$ single excitations in a chromium (III) dimer of C_{2v} symmetry have been derived.[12] We only need to consider the dimer transitions indicated by arrows in Figure 2 for the present discussion. The singlet–triplet excitation $^1A_1 \rightarrow {}^3A_2$ clearly arises through a single-ion mechanism. The two transitions $^3B_2 \rightarrow {}^3A_2$ and $^5A_1 \rightarrow {}^5B_1$ are allowed by both mechanisms. Experimentally, they were both found to be almost completely X-polarized in the corresponding dihydrate.[4] This clearly shows that they are exchange-induced. Theory predicts an intensity ratio $(^3B_2 \rightarrow {}^3A_2)/(^5A_1 \rightarrow {}^5B_1)$ of 5/9. In the dihydrate this ratio was almost exactly observed.[4]

Polarized Absorption Spectra

Figure 3 shows polarized single-crystal absorption spectra of $[(NH_3)_5CrOHCr(NH_3)_5]Cl_5\cdot H_2O$ at three temperatures in the region of the lowest energy $^4A_2{}^4A_2 \rightarrow {}^2E^4A_2$ excitations. The corresponding band positions are listed in Table I. They all shift to lower energy by approximately 5 cm^{-1} between 1.5 and 100 K, as expected.[13] The spectra exhibit a great deal of fine structure at low temperature. There is a pronounced temperature dependence. A number of so-called hot bands, which are completely absent at 1.5 K, increase in intensity with increasing temperature. They can be separated into two groups, one which mainly grows between 1.5 and 25 K and the other one with a strong increase between 25 and 95 K. With reference to Figure 2, these two groups of hot bands are easily assigned to transitions originating in the $^3B_2$ and $^5A_1$ ground levels, respectively, as shown at the top of Figure 3. Their temperature dependence results from the variation of the Boltzmann population factors. All the bands in

---

(9) Linhard, M.; Weigel, M. *Z. Anorg. Allg. Chem.* **1959**, 299, 25.

(10) Huang, N. L. *Phys. Rev. B: Solid State* **1970**, *1*, 3971. Dubicki, L. *Aust. J. Chem.* **1972**, *25*, 739. Van der Ziel, J. P. *Phys. Rev. B: Solid State* **1971**, 4, 2888.

(11) Naito, M. *J. Phys. Soc. Jpn.* **1973**, 34, 1491.

(12) Riesen, H.; Güdel, H. U. *Mol. Phys.* **1986**, *58*, 509.

(13) Di Bartolo, B. *Optical Interactions in Solids*; Wiley: New York, 1968; p 372.

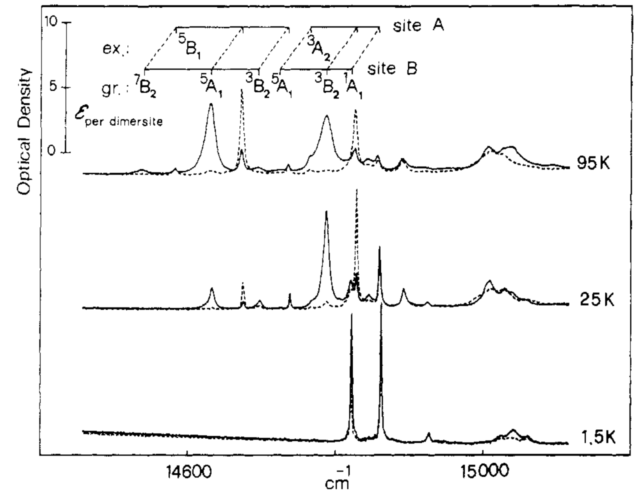

Figure 3. Polarized absorption spectra of $[(NH_3)_5CrOHCr(NH_3)_5]Cl_5{\cdot}H_2O$ at three temperatures: $\vec{E}\|c$ (—), $\vec{E}_{\perp c}$ (- -). Assignments of the bands of the dimer transitions of Figure 2 are given at the top for the two sites A and B.

Table I. Positions and Polarizations of Absorption and Emission Bands in the Region of Low-Energy $^4A_2{}^4A_2 \rightarrow {}^2E^4A_2$ Excitations[a]

absorption			emission		assignt	
energy, cm^{-1}	temp, K	polarizn	energy, cm^{-1}	temp, K	site	
14 821.2	1.5	π			B	$^1A_1 \rightarrow {}^3A_2$
14 820.3	1.5	σ			B	
14 861.5	1.5	π			A	
14 862.2	1.5	σ			A	
14 787.4	43	π			B	$^3B_2 \rightarrow {}^3A_2$
14 827.2	43	σ			A	
14 724	95				B	$^5A_1 \rightarrow {}^3A_2$
14 765	95				A	
14 696	30		14 697.5	1.5	B	$^3B_2 \leftrightarrow {}^5B_1$
14 737	30		14 739	1.5	A	
14 632.5	43	π	14 634.5	1.5	B	$^5A_1 \leftrightarrow {}^5B_1$
14 674.5	43	σ	14 675.5	1.5	A	
14 540	95		14 544	1.5	B	$^7B_2 \leftrightarrow {}^5B_1$
14 583	95		14 585.5	1.5	A	
			14 730.5	1.5	B	$^1A_1 \leftarrow {}^5B_1$
			14 772	1.5	A	

[a] Band assignments are included.

the $^2E^4A_2$ spectrum of $[(NH_3)_5CrOHCr(NH_3)_5]Cl_5{\cdot}H_2O$ appear in pairs with a separation of approximately 41 cm^{-1}. From a comparison with the spectrum of the corresponding dihydrate,[4] it is quite clear that the absorption spectrum of Figure 3 consists of a superposition of two $[(NH_3)_5CrOHCr(NH_3)_5]^{5+}$ spectra. The two spectra correspond to two crystallographically nonequivalent sites A and B. Band assignments to these sites are included in Figure 3. From the relative intensities of the two partners of a given pair of bands we conclude that there is an equal number of sites A and B in the crystal. In the 1.5 K spectrum, which is dominated by the $^1A_1 \rightarrow {}^3A_2$ transition, both sites have a comparable dichroic ratio. In contrast, the hot bands corresponding to $^3B_2 \rightarrow {}^3A_2$ and $^5A_1 \rightarrow {}^5B_1$ are almost completely σ ($\vec{E}\perp c$) and π ($\vec{E}\|c$) polarized for sites A and B, respectively. This is a clear indication that the complexes of sites A and B have different orientations in the crystal. Since we know from the dihydrate that the $^3B_2 \rightarrow {}^3A_2$ and $^5A_1 \rightarrow {}^5B_1$ transitions are X-polarized in the molecular frame (see Figure 1), we deduce from the observed dichroic ratios that the angle between X and the crystal c axis is 90 ± 10° for site A and 0 ± 10° for site B. Site B thus corresponds to the orientation derived from the X-ray diffraction study, whereas the molecules of site A are tilted by 90 ± 10° out of this position. The absorption bands corresponding to the two sites show very different increases of their widths on increasing the temperature. As is seen in Figure 3, both the allowed spin triplet and quintet excitations are approximately 3 times broader for site B than for site A at 95 K. The intensity ratio $(^3B_2 \rightarrow {}^3A_2)/(^5A_1 \rightarrow {}^5B_1)$, corrected for Boltzman populations, in the temperature range 20–100 K is 0.54 ± 0.2 and 0.57 ± 0.2 for sites A and B, respectively. A ratio of 0.56 is expected for purely exchange-induced intensity. We conclude, that this is the dominant mechanism for both sites, in agreement with their almost complete polarization.

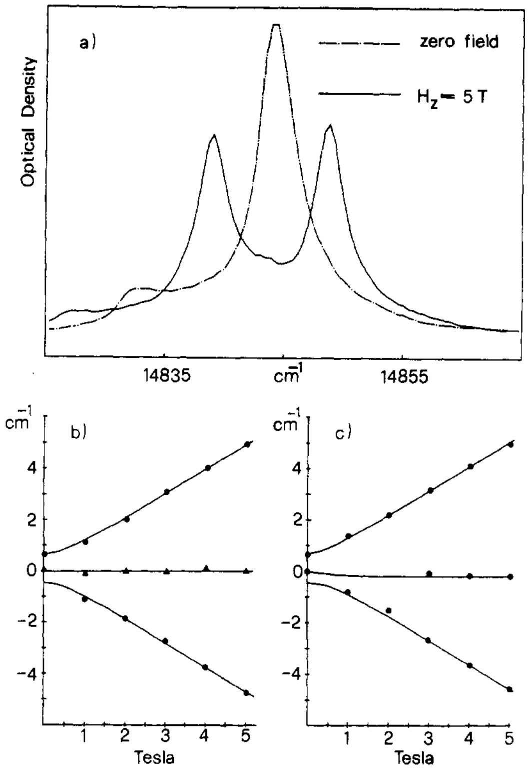

Figure 4. (a) Zeeman absorption spectra at 1.5 K with $\vec{H}\|z$ and $\vec{E} \simeq ((3^{1/2}/2)E_x, (1/2)E_y)$ for the transition $^1A_1 \rightarrow {}^3A_2$ in $[(NH_3)_5CrOH\text{-}Cr(NH_3)_5]Cl_5{\cdot}2H_2O$. (b) Experimental and calculated (eq 3) Zeeman energies of the $^3A_2$ multiplet for $\vec{H}\|z$ at 1.5 K. (▲) $\vec{E}\|z$; (●) $\vec{E} \simeq ((3^{1/2}/2)E_x, (1/2)E_y)$ (ordinate scale: add 14 844.4 cm^{-1}). (c) As in part b but unpolarized and for $\vec{H} = ((1/2)H_x, (3^{1/2}/2)H_y)$.

Table II. Parameters for the $^3A_2$ Dimer Level Derived from the Zeeman Data by Using Eq 3 and 4

		monohydrate	
param	dihydrate	site A	site B
g_x	1.88 ± 0.03		
g_y	2.11 ± 0.04		
g_z	2.05 ± 0.03		
$g_{\|c}$		2.09 ± 0.03	1.89 ± 0.03
$g_{\perp c}$		2.01 ± 0.04	2.08 ± 0.04
D, cm^{-1}	0.07 ± 0.05	0.35 ± 0.2	0.04 ± 0.1
E, cm^{-1}	−0.4 ± 0.1	−0.2 ± 0.1	−0.43 ± 0.2

Zeeman Experiments

Measurements of the Zeeman effect of the sharp absorption lines provide supporting evidence for the relative orientations of sites A and B in the crystal. Detailed Zeeman measurements were performed for the cold $^1A_1 \rightarrow {}^3A_2$ excitations, which are particularly sharp at 1.5 K.

The dihydrate, $[(NH_3)_5CrOHCr(NH_3)_5]Cl_5{\cdot}2H_2O$, in which the complexes are lined up parallel,[4] was used as a reference to determine the molecular anisotropy of the g tensor in the excited state. Figure 4a illustrates the observed effects, and parts b and c of Figure 4 summarize the experimental results for two directions of the applied magnetic field. The data were fitted by the eigenvalues of the effective Hamiltonian[14]

$$\hat{H}_{eff} = D\left[S_z^2 - \frac{1}{3}S(S+1)\right] + E(S_x^2 - S_y^2) + \mu_B(g_xH_x\hat{S}_x + g_yH_y\hat{S}_y + g_zH_z\hat{S}_z) \quad (3)$$

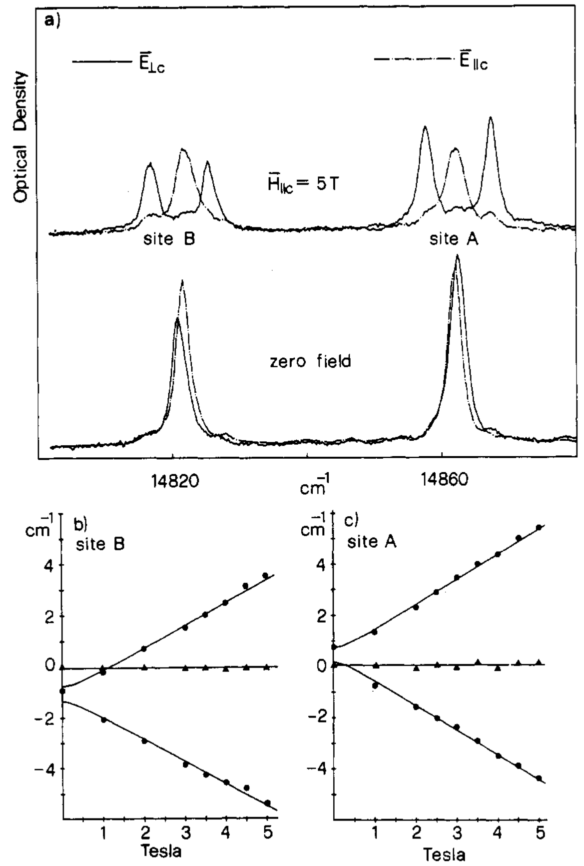

Figure 5. (a) Polarized Zeeman absorption spectra at 1.5 K with $\vec{H} \| c$ in the region of the two ${}^1A_1 \rightarrow {}^3A_2$ transitions in $[(NH_3)_5CrOHCr(NH_3)_5]Cl_5 \cdot H_2O$. (b) Observed and calculated (eq 3 and 4) Zeeman energies of the ${}^3A_2$ multiplet for $\vec{H} \| c$: $\vec{E} \| c$ (▲) and $\vec{E} \perp c$ (●) for site B (ordinate scale: add 14821.2 cm^{-1}). (c) As in part b but for site A (ordinate scale: add 14861.5 cm^{-1}).

The resulting parameters are listed in Table II. The anisotropy of the g values is significant. For our choice of coordinates it is understandable that $|E| > |D|$, because the principal molecular anisotropy is along y.

Figure 5a shows selected experimental Zeeman scans for the monohydrate, and parts b and c of Figure 5 summarize the results with $\vec{H} \| c$ for sites A and B. It is evident from Figure 5 that the behavior of the lines belonging to the two sites in a magnetic field is quite different. A comparison with the dihydrate Zeeman results immediately reveals the relationships

$$g_{\|c}(\text{site A}) = g_z \qquad g_{\|c}(\text{site B}) = g_x \tag{4a}$$

This exactly corresponds to the molecular orientations derived from the polarized absorption spectra. By the use of, in addition, the relationships

$$g_{\perp c}(\text{site A}) \simeq \tfrac{1}{2}(g_x + g_y) \qquad g_{\perp c}(\text{site B}) \simeq \tfrac{1}{2}(g_y + g_z) \tag{4b}$$

and the molecular g_x, g_y, and g_z values of the dihydrate, the experimental Zeeman data of the monohydrate (Figure 5) can be exactly reproduced with eq 3. The corresponding parameters are listed in Table II. There remains no doubt that the CrOCr plane of the complexes in site A does not lie in a plane perpendicular to the c axis as postulated by the X-ray crystal structure study.[5] The tilting angle out of this plane is 90 ± 10°, so that the z axes are parallel to c. From the anisotropy parameters we conclude that the B sites have a surrounding comparable to that of the complexes in the dihydrate. The A site anisotropy parameters, on the other hand, are significantly different, indicating a geometrical distortion of the complex itself or an influence of a different crystal environment. The strength of the exchange coupling is only marginally affected by this. Both sites have very similar exchange parameters, as will be shown in the next section.

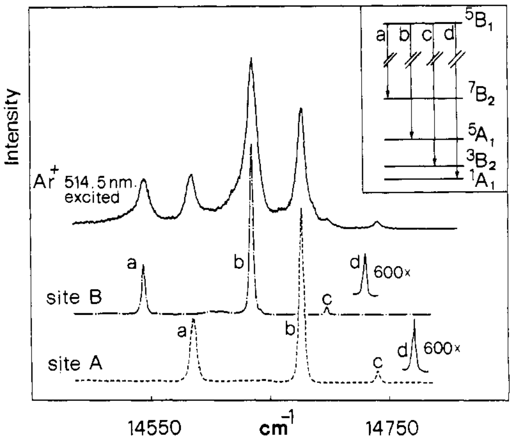

Figure 6. Site-selective luminescence spectra (unpolarized) of $[(NH_3)_5CrOHCr(NH_3)_5]Cl_5 \cdot H_2O$. Sites A and B were excited at 14862 and 14821 cm^{-1}, respectively. The top trace shows a luminescence spectrum excited by the 19430.9-cm^{-1} line of the Ar$^+$ ion laser. Assignments of luminescence lines a–d are given in the insert.

Table III. Ground-State Exchange Parameters of Selectively Excited Dimer Sites in $[(NH_3)_5CrOHCr(NH_3)_5]Cl_5 \cdot H_2O$ at 1.5 K

excitation energy, cm^{-1}	${}^5B_1 \rightarrow {}^5A_1$ luminescence, cm^{-1}	site	J, cm^{-1}	j, cm^{-1}
14 587.5	14 671.5	within the inhomogeneous width of A	−15.3	0.3
14 861	14 674.5		−15.4	0.3
14 862	14 675.5		−15.3	0.3
14 864.8	14 677.8		−15.3	0.3
14 865.8	14 678.3		−15.3	0.2
14 868.6	14 681		−15.2	0.3
14 815.5	14 631	within the inhomogeneous width of B	−15.3	0.3
14 817.2	14 633		−15.3	0.2
14 820.5	14 634.5		−15.3	0.3
14 823	14 637.8		−15.3	0.2
14 824.2	14 639.2		−15.2	0.2
14 834	14 646.9	wing of B	−15.2	0.1
14 844	14 659	between A and B (<1%)	−15.6	0.1
14 854.2	14 667.1	wing of A	−15.4	0.1
14 870.2	14 886.4		−15.0	0.4
14 875	14 691.8		−16.1	0.3
14 892.7	14 709.8	minority (<1%)	−16.1	0.5

Site-Selective Luminescence Spectroscopy

By the use of the ${}^1A_1 \rightarrow {}^3A_2$ transitions at 14862 and 14821 cm^{-1}, respectively, sites A and B can be selectively excited at 1.5 K. The result is shown in Figure 6, together with a luminescence spectrum excited by the green 19430.9-cm^{-1} line of the Ar$^+$ ion laser. The separation of the spectra is seen to be complete at this temperature. The selectively excited luminescence lines are considerably sharper than those excited unselectively by the Ar$^+$ laser line.

All the lines shown in Figure 6 are electronic origins. The four lines of a given site are readily assigned to transitions from the lowest excited dimer level ${}^5B_1$ to the four ground-state levels as shown in the insert of Figure 6. Their positions thus provide very accurate values of the exchange splitting in the ground state. These experimental splittings can be fitted by the eignevalues of the Hamiltonian given in eq 1. The results are collected in Table III.

The luminescence line narrowing observed upon selective excitation (Figure 6) shows that the non selectively excited luminescence lines are inhomogeneously broadened. The same is true for the absorption lines. The wings observed in the top trace of Figure 6 have the same physical origin. The tunable laser technique makes it possible to scan through the inhomogeneously broadened absorption profile of the ${}^1A_1 \rightarrow {}^3A_2$ excitation and obtain selective luminescence spectra within the distribution of site A (or B). It is also possible to selectively excite minority sites

---

(14) Owen, J.; Harris, E. A. In *Electronic Paramagnetic Resonance*; Geschwind, S., Ed.; Plenum: New York, 1972; p 427.

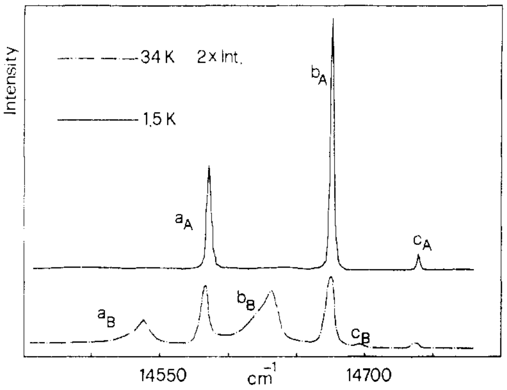

Figure 7. Luminescence spectra for selective excitation (14 862 cm^{-1}) of site A at two temperatures. The lines are denoted as in Figure 6.

in the wings of the main lines A and B, or even sites that are not detectable in the absorption spectrum, contributing less than 1% to the total intensity. Table III contains the results of a few selected majority and minority sites. The observed inhomogeneous broadening and the presence of minority sites demonstrate that the crystal is by no means perfect. The broadening is similar for sites A and B at 1.5 K. However, as shown in Figure 3, the widths of the site B bands increase much more strongly than those of site A.

The ground-state exchange splittings for all the sites resemble the Landé pattern expected for a Heisenberg Hamiltonian rather closely. Accordingly, the biquadratic exchange parameters are small, approximatately 1% of $2J$. Exchange parameter values for the various sites are collected in Table III. These values are very accurate, and they show little variation. In particular, the parameters are the same for the majority sites A and B. This is interesting, because there is a significant difference in the anisotropy parameters D and E between the two sites. We have attributed this difference to a geometrical distortion or a different crystal environment of site A. The exchange parameters are obviously not affected by this. Exchange parameters of minority sites outside the main absorption band profile show deviations of up to ±5% from those of the majority sites. An extreme outsider is the site with a $^5B_1 \rightarrow {}^5A_1$ luminescence energy 34 cm^{-1} above the majority sites A. It has a J value of 16.1 cm^{-1} compared to 15.3 cm^{-1} for the majority sites.

The spectra in Figure 6 clearly show that there is no transfer of excitation energy between the sites at 1.5 K. This is no longer true at higher temperatures, as illustrated in Figure 7. At 34 K selective excitation of site A results in a superposition of luminescence from both sites. Excitation energy is nonradiatively transferred from site A to site B. The process is thermally activated. We have investigated this phenomenona and the possible underlying mechanisms in detail, and a full account of this work is published elsewhere.[12]

Conclusions

We have shown by single-crystal absorption and Zeeman spectroscopy that the published crystal structure of $[(NH_3)_5CrOHCr(NH_3)_5]Cl_5\cdot H_2O$ can only be an approximation. It was determined on the basis of single-crystal X-ray diffraction data and refined to a R value of 0.077. A structural phase transition between room temperature and 1.5 K can be ruled out as a reason for the discrepancy between the spectroscopic and X-ray results on the basis of the room-temperature absorption spectrum. The existence of two crystallographically nonequivalent sites is clearly established by the spectroscopy, and the orientation of both sites in the crystal determined. Site B corresponds to the X-ray position, whereas site A is tilted by 90 ± 10° around the molecular y axis from that orientation. High-resolution optical spectroscopy proves to be a very sensitive structural probe in this situation. In addition, it allows the determination of molecular parameters for each individual site in the crystal. The main focus in this study was on the ground-state exchange splitting of the $[(NH_3)_5CrOHCr(NH_3)_5]^{5+}$ units. The exchange parameters of the majority sites are in exact agreement with those determined on the deuterated compound at 30 K by another spectroscopic technique, inelastic neutron scattering (INS).[15] The spectral resolution of the optical spectroscopic results at 1.5 K presented here is approximately 1 order of magnitude better than the INS resolution in ref 15. In contrast to INS, optical spectroscopy provides selectivity. It has the additional advantage that the transfer of excitation energy can be investigated, thus providing information about intermolecular interactions. It turns out to be a highly sensitive and selective technique for probing both electronic excitations and structural properties.

Acknowledgment. We thank N. Furer and P. Küng for their assistance with the synthesis and crystal growth. Financial support by the Swiss National Science Foundation is gratefully acknowledged.

Registry No. $[(NH_3)_5CrOHCr(NH_3)_5]Cl_2\cdot H_2O$, 15629-41-1.

---

(15) Güdel, H. U.; Furrer, A. *Mol. Phys.* **1977**, *33*, 1335.

Contribution from the Service d'Etudes Analytiques and the Département de Recherche Fondamentale,
Centre d'Etudes Nucléaires de Grenoble, 85 X, 38041 Grenoble Cedex, France

Desorption Chemical Ionization Mass Spectrometry via Electron Capture of Hydrolytically Labile Titanium Porphyrins

E. Forest,[†] J. C. Marchon,*[‡] J. Ulrich,[†] and H. Virelizier[§]

Received February 12, 1986

A comparison of electron impact ionization (EI), fast atom bombardment (FAB), and desorption chemical ionization (DCI) mass spectrometry of dihalogenotitanium(IV) porphyrins shows that DCI in the electron capture mode is uniquely suited to the production of abundant molecular ions for this class of hydrolytically labile coordination complexes.

The mass spectrometric characterization of metalloporphyrin complexes[1] is often plagued by the cleavage of their axial metal–ligand bonds. Thus, the highest peaks in the mass spectra of five- and six-coordinate porphyrin complexes usually correspond to the molecular ion of the four-coordinate metalloporphyrin or to that of a hydrolytically produced oxo complex. The difficulties in obtaining accurate structural and molecular weight information

---

[†] Service d'Etudes Analytiques (CEA/IRDI), CEN de Grenoble.

[‡] Département de Recherche Fondamentale (DRF/LCH), CEN de Grenoble.

[§] Service d'Etudes Analytiques (CEA/IRDI), CEN de Saclay.

(1) For recent advances in this field, see: (a) Kurlansik, L.; Williams, T. J.; Strong, J. M.; Anderson, L. W.; Campana, J. E. *Biomed. Mass Spectrom.* **1984**, *11*, 475–481. (b) Sundararaman, P.; Gallegos, E. J.; Baker, E. W.; Slayback, J. R. B.; Johnston, M. R. *Anal. Chem.* **1984**, *56*, 2552–2556. (c) Fukuda, E. K.; Campana, J. E. *Anal. Chem.* **1985**, *57*, 949–952. (d) Chait, B. T.; Field, F. H. *J. Am. Chem. Soc.* **1984**, *106*, 1931–1938. (e) Freas, R. B.; Campana, J. E. *Inorg. Chem.* **1984**, *23*, 4654–4658.